How effectively do carbon nanotube inclusions contribute to theelectromagnetic performance of a composite material? Estimation criteria from microwave and terahertz measurements

Shuba, Mikhail; Yuko, Dzmitry; Kuzhir, Polina; Maksimenko, Sergey; Kanygin, Mikhail; Okotrub, Alexander; Tenne, Reshev; Lambin, Philippe

Published in:
Carbon

DOI:
10.1016/j.carbon.2017.12.067

Publication date:
2018

Document Version
Peer reviewed version

How effectively do carbon nanotube inclusions contribute to the electromagnetic performance of a composite material? Estimation criteria from microwave and terahertz measurements

M. V. Shuba[a,*], D. I. Yuko[a], P. P. Kuzhir[a], S. A. Maksimenko[a], M. A. Kanygin[b], A.V. Okotrub[b,c], R. Tenne[d], Ph. Lambin[e]

[a] *Institute for Nuclear Problems, Belarus State University, Bobruiskaya 11, 220050 Minsk, Belarus*
[b] *Nikolaev Institute of Inorganic Chemistry, SB RAS, 3 Acad. Lavrentiev av., 630090 Novosibirsk, Russia*
[c] *Novosibirsk State University, 1 Pirogova str., 630090 Novosibirsk, Russia*
[d] *Department of Materials and Interfaces, Weizmann Institute of Science, Rehovot 76100, Israel*
[e] *Physics Department, Université de Namur, 61 Rue de Bruxelles, B-5000 Namur, Belgium*

Abstract

Screening effect in finite-length carbon nanotubes (CNT) and their agglomerates hinders significantly the electromagnetic interaction in composite materials. Screening effect is strong in the microwave range, and it decreases with increasing frequency resulting in a strong frequency dependence of the effective conductivity of the composite. Since screening effect is rather small in the terahertz range, the effective conductivity in this range is determined directly by the intrinsic conductivity of the inclusions. The ratio of the microwave to terahertz effective conductivities was proposed as a parameter to estimate how effectively carbon nanotube inclusions contribute to the electromagnetic performance of composite materials in the microwave range. CNT film was considered as a material where maximal possible interaction of the CNTs with EM field occurs. Single-walled CNT films and CNT-based composite materials, as well as hybrid film comprising mixtures of WS_2 nanotubes and CNTs were fabricated and measured in the microwave and terahertz ranges. The electromagnetic field interaction with the inclusions has been estimated for all the samples fabricated.

*Corresponding author. Tel: +375 17 2264223. Fax: +375 17 2265124.
Email address: mikhail.shuba@gmail.com (M. V. Shuba)

1. Introduction

High conductivity and very high aspect ratio of carbon nanotubes (CNT) cause their effective interaction with electromagnetic (EM) radiations [1, 2, 3, 4, 5, 6, 7, 8]. Many interesting effects in CNTs have been recently predicted and demonstrated, including: propagation of slowed-down surface waves [8], localized plasmon (antenna) resonance in the terahertz range [9, 4], screening effect in microwave and radio-frequency ranges [5, 10], strong near-field enhancement [5, 11], and Purcell effect [12]. CNTs have been proposed as elements for different integrated circuits and electromagnetic devices, such as transmission lines [8, 7], nanoantennas [13, 14, 15], interconnects [16, 17], terahertz detectors and emitters [18]. Moreover, CNTs have real perspective applications as inclusions in composite materials for different electromagnetic applications [11, 19, 20, 21]. A large variety of CNT-based composites have been produced and investigated during the past two decades [22, 19]. They aimed at obtaining the maximal electrical conductivity of the composite material with minimal concentration of inclusions. This can be achieved by a suitable choice of the CNT geometry [10] and homogeneous distribution of the CNTs in the host matrix [23, 24].

Many efforts have been made to achieve a homogeneous dispersion of CNTs in the host matrix [22, 25, 26, 27, 28]. To that end, different strategies have been applied, including melt mixing [23], ultrasonic treatment, CNT cutting [29], functionalization of CNTs [28, 22, 25, 27], or additional inclusions preventing CNT aggregation [30]. Though all these methods help to improve CNT dispersion, additional side effects may partly prevent the achievement of the most effective interaction of the CNT inclusions with an electromagnetic field. For instance, functionalization of the CNTs may increase intertube contact resistance [26, 28]; ultrasonic and chemical treatment may lead to the CNT cutting [31]. Different techniques are used to estimate the morphology of the prepared composites, among which terahertz spectroscopy [32, 33], rheological measurements [34], microscopic observations [23, 24], X-rays diffraction tests [35], and dc-electric conductivity measurements [23, 24].

Electromagnetic shielding performance of a composite slab is usually evaluated by its shielding effectiveness (SE) that depends on the effective permittivity of both the sample and surrounding media and on the thickness of the sample as well. SE parameters are determined by interference effects in the slab and impedance mismatch between the surrounding media

and the sample.

Currently, there is no criteria which can assess how effectively CNT inclusions contribute to the electromagnetic performances of a composite material, and how far the electrical conductivity of the fabricated composite is from maximal possible conductivity at the given CNT volume fraction. The major cause hindering electromagnetic interaction is a screening effect in the individual inclusions or their aggregates. Screening effect is maximal in a wide range, from radiofrequency to microwave, and is minimal in the terahertz range [5, 10]. By comparing the conductivity of a CNT film and a CNT-based composite material in the terahertz and microwave (or static) ranges, we formulate a criterion for the evaluation of the quality of the CNT-based material with respect to its electromagnetic performance. We also propose to compare the conductivity of CNT composites with that of CNT films, where the EM response of CNTs is as large as possible.

2. Theoretical background

In this section we present theoretically a criterion that characterizes how effectively CNT-inclusions interact with the EM field. Though the consideration is carried out for the case of single-walled CNTs, it remains true for composite comprising multi-walled CNTs and bundles of single-walled CNTs.

The conductivity spectra of CNT composite materials have a broad terahertz peak[1, 2, 3, 4] due to a finite-length effect [15]. The peak frequency f_p increases with decreasing CNT length [9]. For further consideration we assume that the CNTs are long enough, so that $f_p < \nu/2\pi$, where $\nu = \tau^{-1}$; τ is the electron relaxation time. This condition is satisfied for CNTs with length $L \geq 1$ μm and $\tau < 50$ fs; it provides non-resonant interaction of CNT with the electromagnetic wave below 3 THz. Calculations are performed here for undoped metallic CNTs. Since doped semiconducting tubes have conductivity comparable to that of metallic CNTs [36], equivalent results would be obtained with doped semiconducting CNTs.

2.1. Individual carbon nanotube

In the terahertz and subterahertz ranges, the surface conductivity of the metallic single-walled CNT is determined mainly by intraband electron transitions and described by the

Drude formula [8]:

$$\sigma_{\rm cn} = \frac{2ie^2 v_F}{\pi^2 \hbar R(\omega + i\nu)}\,, \tag{1}$$

where v_F is the Fermi velocity, $v_F \simeq 10^6$ m/c; R is the CNT radius; $\omega = 2\pi f$ is the angular frequency, f is the frequency, e is the charge of electron; $\hbar$ is the reduced Planck constant.

As an example, the conductivity spectrum for zigzag (12,0) CNT is shown in Fig. 1(a). One can divide the spectrum in two regions: (i) the low frequency region, $f < \nu/4\pi$, where the conductivity is mainly real and equal to the static conductivity; (ii) the higher frequency region, $f > \nu/4\pi$, where the conductivity is complex and frequency dependent.

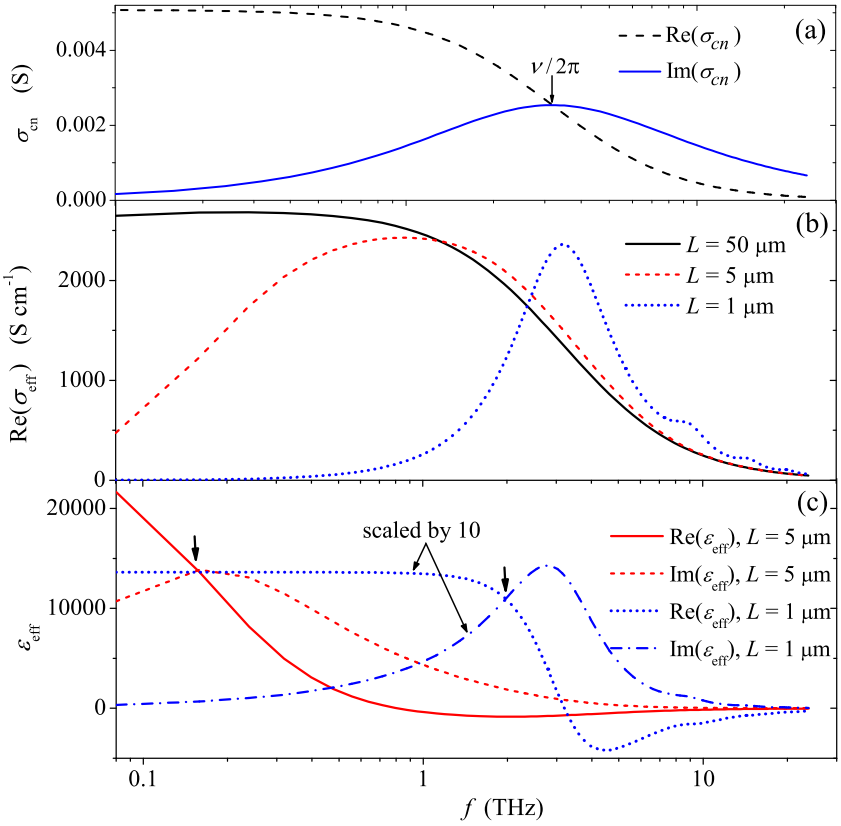

Figure 1: (a) Spectrum of the axial surface conductivity of metallic zigzag (12,0) CNT; (b) The effective conductivity spectra of the composite materials comprising identical (12,0) CNTs with length $L \in \{1, 5, 50\}\mu$m at the same CNT volume fraction $F = 5\%$. (c) Real and imaginary parts of the effective permittivity of the composites mentioned in (b) at $L \in \{1, 5\}\mu$m. Vertical arrows in (c) indicate the frequencies f_s which satisfy the equality $\mathrm{Im}(\varepsilon_{\rm eff} - \varepsilon_{\rm h})/\mathrm{Re}(\varepsilon_{\rm eff} - \varepsilon_{\rm h}) = 1$. In calculations, we used $\tau = 50$ fs.

Let an isolated single-walled CNT of length L and radius R, and aligned parallel to the

z axis of a Cartesian coordinate system, occupies the region $z \in (0, L)$. The CNT is exposed to an incident field with z-component $E_z = E_z^0 exp(-i\omega t)$. The scattered EM field is induced by the axial surface current excited in the CNT. The surface current density $j(z)$ depends both on the tube conductivity $\sigma_{\rm cn}$ and the axial component of the total electric field $E_z^{\rm tot}$ on the CNT surface:

$$j(z) = \sigma_{\rm cn} E_z^{\rm tot}(z)\,, \tag{2}$$

where $E_z^{\rm tot} = E_z^0 + E_z^{\rm sc}$, $E_z^{\rm sc}$ is the axial component of the field scattered by the CNT.

Let us introduce the effective surface conductivity of the CNT

$$\sigma_{\rm cn}^{\rm (eff)} = \frac{\sigma_{\rm cn}}{L} \int_0^L \frac{E_z^{\rm tot}(z)}{E_z^0(z)} dz\,. \tag{3}$$

Following [10], one can identify three different regimes of CNT interaction with the electromagnetic field: quasi-static ($f \ll f_p$), intermediate ($f \approx f_p$), and dynamic regimes ($f \gg f_p$).

In the quasi-static regime, due to the polarization of finite-length CNT, the scattering (depolarizing) field partly compensate the z-component of the incident field resulting in the screening effect, i.e. $E_z^{\rm tot} \ll E_z^0$, and consequently $|\sigma_{\rm cn}^{\rm (eff)}| \ll |\sigma_{\rm cn}|$. The screening effect is stronger for shorter tubes and low frequencies. It gets weaker as frequency increases. As a result, the value of $\sigma_{\rm cn}^{\rm (eff)}$ increases with frequency in the range from 0 Hz up to the frequency f_p.

In the dynamic regime, the screening effect is absent, i.e., $E_z^{tot} \approx E_z^0$, and consequently $\sigma_{\rm cn}^{\rm (eff)} \approx \sigma_{\rm cn}$. The same is true for the intermediate regime at high electron relaxation rate, i.e. at the condition of $f_p < \nu/2\pi$.

2.2. Carbon nanotube based composite

Let us now consider a composite material where the CNT inclusions are randomly dispersed and randomly oriented in the dielectric matrix with the relative effective permittivity ε_h. For simplicity, we assume that tubes are isolated from each other and there is no electromagnetic interaction between them. We use adapted the Waterman-Truell formula to

estimate the effective relative permittivity of this composite material [4]

$$\varepsilon_{\text{eff}}(f) = \varepsilon_h(f) + \frac{1}{3\epsilon_0}\sum_m \int_0^\infty \alpha_m(f,L) N_m(L) dL\,, \tag{4}$$

where $\varepsilon_0 = 8.85 \times 10^{-12}$ F m^{-1}; the function $N_m(L)$ describes the number density of the CNTs of type m with radius R_m and length L. The factor 1/3 in equation (4) is due to the random orientations of the CNTs; and

$$\alpha_m(f,L) = \frac{R_m}{f E_z^{(0)}} \int_0^L j(z) dz \tag{5}$$

is the axial polarizability calculated using the integral equation approach [37]. We shall describe the contribution from the inclusions to the total conductivity of the composite material by the effective conductivity

$$\sigma_{\text{eff}} = 2\pi f \varepsilon_0 (\varepsilon_{\text{eff}} - \varepsilon_h)\,. \tag{6}$$

Let us note that the frequency dependence of σ_{eff} in the range $(0,f_p)$ is explained in some papers by Drude-Smith model [38, 39]. However, application of this model is not justified, as it cannot explain a variation of the frequency dependence $\sigma_{\text{eff}}(f)$ with the CNT concentration in the network (see Sec. 3).

Fig. 1(b,c) shows the spectra of $\text{Re}(\sigma_{\text{eff}})$, $\text{Re}(\varepsilon_{\text{eff}})$, and $\text{Im}(\varepsilon_{\text{eff}})$ calculated for composites comprising identical metallic single-walled CNTs at different, but consistent within each sample, CNT lengths $L \in \{1, 5, 50\}\mu$m and the same nanotube volume fraction $F = 2\pi R^2 L \widetilde{n}$, where $\widetilde{n}$ is a number density of the tubes of length L and radius R. The spectrum of $\text{Re}(\sigma_{\text{eff}})$ for the longest tubes ($L = 50$ μm) follows the Drude law, whereas the spectra for shorter tubes with $L = 5$ μm and $L = 1$ μm have a terahertz peak at $f_p = 0.9$ and 3 THz, respectively.

Let us note that for all composites in Fig. 1(b), the value of $\text{Re}(\sigma_{\text{eff}})$ is approximately the same at the peak frequency f_p and approximately equal to that found for "infinitely long" tubes ($L = 50$ μm). This is due to the absence of the screening effect at frequency f_p in the intermediate regime where $E_z^{\text{tot}} \approx E_z^0$. Indeed, after substitution of (2) into (5), (5) into (4), and (4) into (6), taking into account that $E_z^{\text{tot}} \approx E_z^0$, for composite with identical CNTs at frequency f_p, we obtain

$$\sigma_{\text{eff}}(f_p) \approx \frac{2}{3}\pi R L \widetilde{n} \sigma_{\text{cn}}(f_p) = \frac{F}{3R}\sigma_{\text{cn}}(f_p)\,. \tag{7}$$

One can conclude from (7) and Fig. 1(b) that at the same volume fraction of CNTs (i) the effective conductivity does not depend on the tube length at frequency f_p, and (ii) the value of $\mathrm{Re}[\sigma_{\mathrm{eff}}(f_p)]$ is the maximal value of the real part of the effective conductivity in the range $f < f_p$. The value $\mathrm{Re}[\sigma_{\mathrm{eff}}(f_p)]$ practically does not depend on whether the nanotubes are or not in the contact with each other. Consequently, this value does not depend on the method of composite preparation and distribution of the tubes in the matrix. It is worth reminding that all this is true as long as $f_p < \nu/2\pi$.

These conclusions give us a criterion to estimate the quality of the prepared composite material. Let us introduce the following ratio

$$g(f, f_0) \equiv \frac{\mathrm{Re}[\sigma_{\mathrm{eff}}(f)]}{\mathrm{Re}[\sigma_{\mathrm{eff}}(f_0)]}\,, \tag{8}$$

as a parameter showing the contribution of the inclusions to the electromagnetic performance of the prepared composite. f_0 in (8) is a frequency at which the screening effect within inclusions or aggregates of inclusions can be neglected. For the composites considered in Fig. 1(b,c), the screening effect is small in the range $f_0 \in (f_s, f_p)$, where f_s is a frequency at which the equality $\mathrm{Im}(\varepsilon_{\mathrm{eff}} - \varepsilon_{\mathrm{h}})/\mathrm{Re}(\varepsilon_{\mathrm{eff}} - \varepsilon_{\mathrm{h}}) = 1$ is true; f_s is indicated by vertical arrows in Fig. 1(c).

For hypothetical composite material comprising "infinitely-long" homogeneously distributed CNTs, from (8), one gets $g = 1$, while for realistic composite, it is expected that $g < 1$. The higher the value g is, the more effectively the inclusions contribute to the electromagnetic response of the composite.

Realistic CNT-based composites are complex systems where electron transport is caused by intrinsic conductivity of the CNTs and intertube electron tunneling [40, 41]. Moreover, the electromagnetic interaction between nanoparticles takes place [42]. All these microscopic effects determine the charge and the total field distribution along the CNTs. According to eq. (2), the total field is responsible for the current induced in the CNT network. If the total field is less than the incident field, one can talk about screening effect. Thus, microscopic effects influence the effective conductivity via the total field and consequently via the screening effect.

Let us notice that the intrinsic conductivity of the CNTs can change when they form

bundles. This occurs through additional electron scattering by phonons in the adjacent tubes of the bundle. Similar phenomena have been reported for multilayer graphene structures [43]. However, this effect does not modify the frequency dependence of the tube conductivity in the range $f \ll \nu$. As shown in recent experiments [44, 45] (see also Fig. 3(a)), the effective conductivity of films containing long-length bundled single-walled CNTs has weak frequency dependence below 1 THz. Therefore, we attribute the strong frequency dependence of the observed value of $\mathrm{Re}(\sigma_{\mathrm{eff}})$ to screening effect in the inclusions and their agglomerates.

It is expected that the parameter g depends on the volume fraction F of the CNTs. At low F, microwave effective conductivity of the composite material is determined mainly by the electromagnetic response of individual tubes, i.e. tube polarizability [46, 40]. Then, the screening effect is strong and the parameter g is small. When F increases, nanotubes start to interconnect and form a highly conductive network that significantly increases the effective conductivity of the composite [46, 40], which decreases the screening effect due to the intertube electron tunneling. As a result, g increases with F.

For diluted CNT composites ($F \ll 1$), we propose to use a normalized parameter

$$g_0(f, f_0) \equiv \frac{g(f, f_0)}{g_{\mathrm{film}}(f, f_0)}\,, \tag{9}$$

where g_{film} is the parameter g for a pure film containing the very same kind of CNTs as the composite material does. A CNT film has the largest possible density of CNT network where screening effect in each tube is minimized due to charge transfers through the tunneling contacts between adjacent CNTs. Then for any composite material the following equality $g_0(f, f_0) \leq 1$ remains true.

The parameter g_0 characterizes the dispersion of the CNTs in the composite. If the tubes are aggregated, forming dense particle, the depolarizing field within each aggregate leads to the screening effect resulting in the low value of the parameter g_0. The composite material with $g_0 = 1$ has the highest possible electromagnetic performance at the given volume fraction of the inclusions. The smaller g_0 with respect to unity is, the less effectively the inclusions are involved in the electromagnetic interaction.

To calculate the parameters g and g_0, one needs to know the frequency f_0. Our estimations made for the composite comprising single- and multi-walled CNTs [10, 47] show that

for long tubes ($L > 1$ μm), the screening effect is rather weak at 1 THz. This is supported by the experimental data showing linear concentration dependence of the absorption at 1 THz for CNT-based composite [32]. Therefore, one can apply $f_0 = 1$ THz in (8) and (9).

Parenthetically, for CNT-based composites at high CNT loading, the real part of the effective conductivity remains practically constant in the range (0,30) GHz [48, 38]. Therefore, the values of g and g_0 practically do not depend on the frequency in this range.

In the next sections, we present terahertz and microwave conductivity data for fabricated CNT films and CNT-based composites and evaluate the parameters g and g_0 at 30 GHz for them.

3. Experimental results

3.1. Materials, sample preparation, and measurements

In our experiment we used purified single-walled CNTs (OCSiAl Inc.) produced by CVD process with diameters of 1.8-2.2 nm, and a purity exceeding 95%.

A free standing CNT film was prepared via the vacuum filtration technique [49]. Briefly, a CNT material was dispersed by ultrasonic treatment (Ultrasonic device UZDN-2T, 44 kHz, maximum power) for 1 hour in an aqueous suspension with 1% sodium-dodecylsulfate (SDS). The suspension was centrifuged at $8000g$ for 20 minutes and then filtrated through a cellulose nitrate membrane filter (0.2 μm pore size) causing a CNT film to collect on the filter. This film was washed with distillate water to remove the surfactant. The filter paper was dissolved by acetone and the CNT film was transferred onto a frame with a hole of 8 mm in diameter. Film thickness was 500 nm. Typical scanning electron microscopy (SEM) image of the film is represented in Fig. 2(a).

The filtration method was also used to fabricate 700 nm thin film comprising short CNTs ($L < 500$ nm). To obtain short tubes, purified single-walled CNTs were cut by ultrasonic treatment in a mixture of nitric and sulfuric acids at low temperature [50].

Polystyrene composite with 1 wt.% of single-walled CNTs was prepared by forge rolling method [51]. CNT material was dispersed in toluene by mechanical stirring for an hour. Polystyrene was mixed with CNT-toluene suspension by stirring until complete dissolution of polymer. The suspension was under ultrasonication treatment for 5 min and then stirred

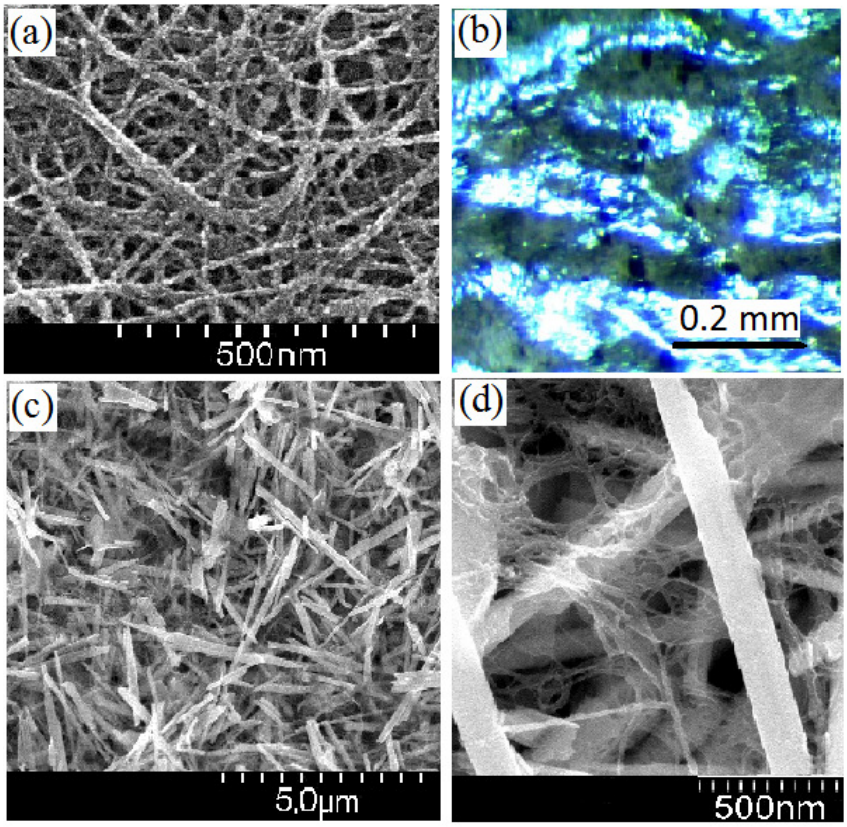

Figure 2: (a) SEM image of the single-walled CNT film; (b) Optical image of the polystyrene composite film with 1 wt.% of single-walled CNTs. (c,d) The SEM images of hybrid CNT/INT film at CNT density of 11 g cm^{-3}. The thick white tubes are INTs and the thin white curves are the single-walled CNTs.

for 2 h. Obtained composite slush was applied over aluminium foil plate and dried at ambient conditions for 3 h to the viscous state. Then the sample was under 20 cycles of forge-rolling. The obtained CNT-based polymer film was dried under a light load at room temperature for 12 h. The film thickness was 0.2 mm. Optical image of the film is represented in Fig. 2(b). The black spots with the size of less than 20 μm indicate CNT agglomerates in Fig. 2(b).

To study the influence of the tube density on the EM field interaction with the inclusions, we fabricated hybrid films consisting of well-dispersed and non-aggregated CNTs mixed with non-conductive inorganic WS_2 nanotubes (INT). For these films, we used non-purified High Pressure Carbon Monoxide single-walled CNTs with diameters of 0.8-1.2 nm (NanoIntegris Inc.). INTs have lengths 1-10 μm and diameters 20-180 nm; they are semiconducting with

a bandgap of 2 eV and transparent at microwave and terahertz frequencies. The details of INT synthesis can be found elsewhere [52].

CNTs were dispersed in 1 wt.% aqueous solution of SDS and then centrifugated at $10000g$ for 15 min. Strong centrifugation leads to purification of the tubes and removes aggregated CNTs. INT material was dispersed in 1 wt.% SDS aqueous solution for 30 min and then immediately centrifugated for 15 min at $300g$. The suspensions of CNTs and INTs were mixed in different proportions and then filtrated to obtain thin films with thickness between 0.7 and 12 μm. The quantity of INTs and CNTs in suspensions before mixing was controlled using visible spectroscopy (RV2201 spectrophotometer, SOLAR, Belarus). In this way, we obtained films with different volume fractions of CNTs. SEM images of the hybrid film show that thin CNTs are dispersed evenly between thick INTs (see Fig. 2(c,d)). The films were transferred to 10 μm thick PTFE substrate for terahertz and microwave measurements. Film thickness was measured with the profilometer Veeco Dektak 6 M.

Transmittance spectra of the CNT film was obtained in the ranges 0.1-2 THz, 2-270 THz, and 270-1000 THz using terahertz time-domain spectroscopy (EKSPLA, Lithuania), a Fourier-transform infrared spectrometer Vertex 70 (Bruker), and an RV2201 spectrophotometer (ZAO SOLAR, Belarus), respectively. The conductivity spectrum of the CNT film was determined from its transmittance spectrum via the Kramers-Kronig relations [6].

The complex transmission of the samples was measured under normal incidence in the range 0.2–1.5 THz using time-domain terahertz spectrometer (EKSPLA, Vilnius Lithunia). The spectrum of the sample conductivity was calculated by means of the Fourier transform of the measured time-domain signal and application of the Fresnel equations for dielectric slab [53]. The microwave conductivity measurements at 30 GHz were performed by waveguide method [54, 55] using a scalar network analyzer R2-408R (ELMIKA, Vilnius, Lithuania).

3.2. Results and discussion

Fig. 3(a) shows the effective conductivity spectrum of the CNT film. The spectrum has a peak at $f_p = 1.5$ THz. Choosing $f_0 = 1$ THz, we obtain at 30 GHz: $g(30\text{GHz}, 1\text{THz}) = 0.64$. This means, roughly speaking, that the effective medium at 30 GHz has only 64% of quasi-free electrons with respect to the total number of quasi-free electrons in the CNT film.

Parameter g for the CNT film depends on the type and geometry of the inclusions. It is shown in [47] that frequency dependence of the CNT film conductivity gets stronger as CNT length decreases. This tendency is demonstrated in Fig. 3(b) for thin film comprising short CNTs. From Fig. 3(b) we get $g(30\text{GHz}, 1\text{THz}) = 0.33$. So, the parameter g decreases as the tube length decreases.

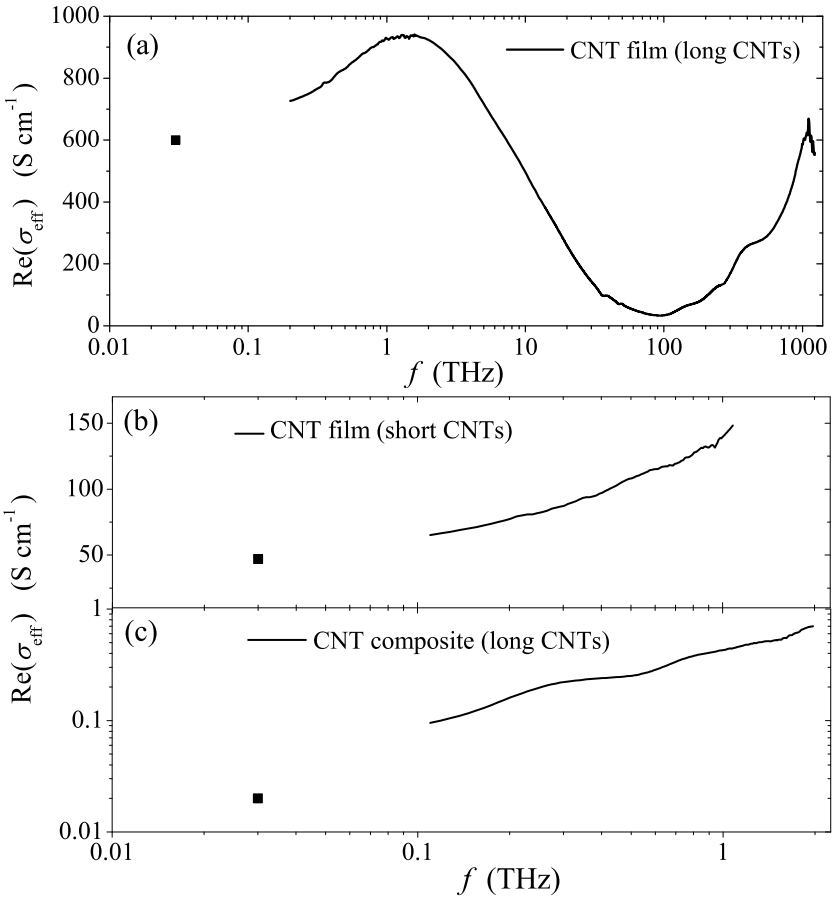

Figure 3: Frequency dependence of $\text{Re}(\sigma_{\text{eff}})$ for the film comprising (a) long, and (b) short CNTs, and (c) for CNT-polymer composite containing 1 wt% of long CNTs. Black square symbols indicate the conductivity of the samples at 30 GHz.

In order to show how the parameters g and g_0 vary with the CNT density, we measured the conductivity spectra of the CNT/INT films at different CNT volume fractions (see Fig. 4(a)). We roughly estimated the volume fraction as the ratio of CNT density ρ to the density of graphite $\rho_0 = 2.2$ g/cm^3. Fig. 4(b) demonstrates the dependence of the parameters $g(30\text{GHz}, 1\text{THz})$ and $g_0(30\text{GHz}, 1\text{THz})$ on the CNT volume fraction. As shown in Fig. 4(b)

both values g and g_0 decrease as CNT volume fraction decreases. The less the ratio ρ/ρ_0, the stronger CNT separation in the composite is, and the stronger the screening effect within each CNT is. It should be noticed that CNT/INT films do not contain agglomerated CNTs. As a result, the CNT interaction with the EM field is high ($g_0 > 75\%$, $g > 25\%$) even at low volume fraction of CNTs ($\rho/\rho_0 \approx 1\%$).

We also found an increase of the value of g with CNT concentration from the data given in [29]. We estimated from the broad band conductivity spectra of polymethylmethacrylate composite with embedded multi-walled CNTs (Fig. 3 of [29]) that $g(30\text{GHz}, 1\text{Thz}) \approx 0.001; 0.011; 0.05$ at CNT loading of 0.25; 1; 2 wt.%, respectively.

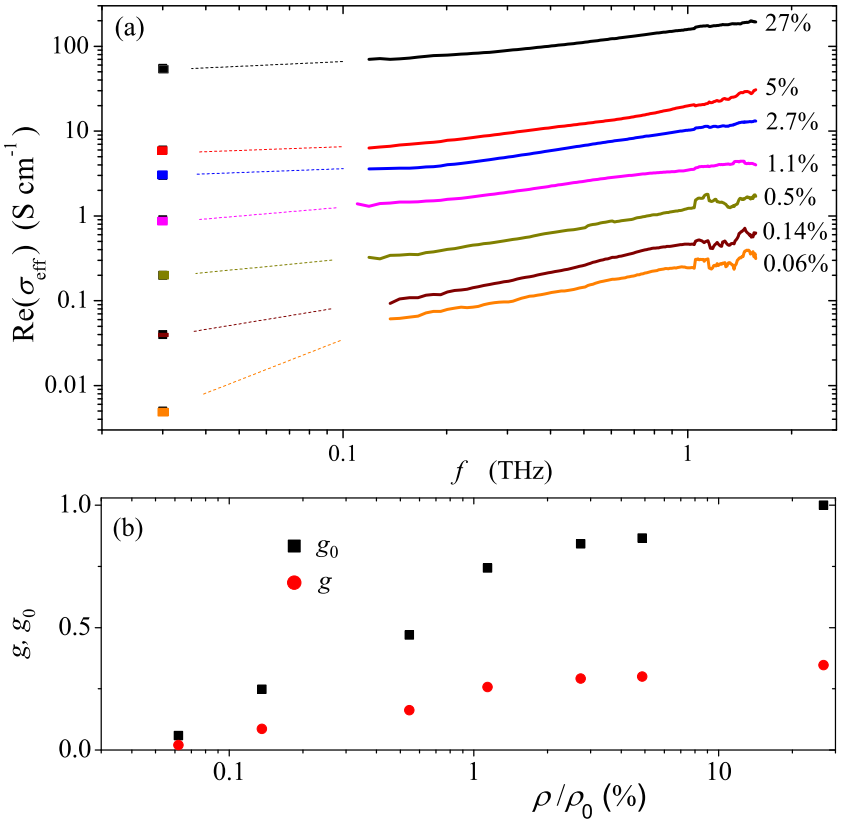

Figure 4: (a) Frequency dependence of $\text{Re}(\sigma_{\text{eff}})$ for the CNT/INT film at different CNT volume fractions $\rho/\rho_0 \in \{0.06, 0.14, 0.5, 1.1, 2.7, 5\}\%$; ρ is a density of CNTs; $\rho_0 = 2.2$ g/cm^3 is the density of graphite; for pure CNT film $\rho/\rho_0 = 27\%$; (b) The parameters $g(30\text{GHz}, 1\text{THz})$ and $g_0(30\text{GHz}, 1\text{THz})$ calculated from data presented in (a) versus ρ/ρ_0.

In order to show the influence of agglomeration on the parameters g and g_0, we measured

the conductivity spectrum of the polystyrene composite with wt 1 wt% of the CNT inclusions (see Fig. 3(c)). As shown in Fig. 3(c), the frequency dependence of the conductivity is very strong. From the data presented in Fig. 3(c), we obtain $g(30\text{GHz}, 1\text{THz}) = 0.045$ and $g_0(30\text{GHz}, 1\text{THz}) = 0.071$. This means that the contribution of the CNTs to the EM response of the composite material obtained is about 7% of that we got for the CNT film. This value of g_0 is about 10 times smaller than that we obtained for the CNT/INT film at approximately the same CNT volume fraction. The reason is that the CNTs are mainly aggregated in the polymer composite, and, consequently, the screening effect within each agglomerate hinders significantly the interaction between the EM field and CNTs. Note, the strong difference in the frequency dependence of the optical density between CNT film and CNT/polyethyelene composite was observed in the subterahertz range (see Fig. 2 in [56]).

The screening effect is rather strong in finite-length multi-walled CNTs [10]. From the conductivity spectrum of the polyethylene based composite with 10 wt% of multi-walled CNTs (Fig. 9 in [57]), we extracted $g(30\text{GHz}, 300\text{GHz}) = 0.04$, that demonstrates low efficiency of the interaction between the CNTs and EM field.

Though we applied g and g_0 for evaluation of CNT-based composite, these parameters can be applied to any type of composite material, where the screening effect is the main factor hindering the electromagnetic interaction.

4. Conclusion

We show theoretically that the effective conductivity of single-walled CNT composite at frequencies close to 1 Thz is determined mainly by the intrinsic conductivity of the CNTs with length $> 1\mu$m. The microwave effective conductivity strongly depends on the screening effect in both the individual CNTs and CNT aggregates. We propose to use a parameter g, defined as the ratio of the microwave to terahertz conductivities, to estimate how effectively carbon nanotube inclusions contribute to the electromagnetic performances of a composite material in the microwave range. Also, we propose to consider a CNT film as a reference material where the strongest possible interaction of the CNTs with the EM field occurs. The ratio of the parameters g of the composite material to that of the CNT film gives us another performance parameter g_0, which is helpful to know how far the EM response of the

composite is from the maximal possible one.

Thin films comprising long and short single-walled CNTs and diluted (1 wt.%) polymer CNT composites were fabricated. The effective conductivities of the samples were measured in the microwave (30 GHz) and terahertz (0.2–1.5 THz) ranges. The parameters g and g_0 for the prepared composite materials were found to be of several percents. The same values of g was extracted from the data taken in the literature. This indicates very low efficiency of the field interaction with CNT inclusions due to aggregation effects in the polymer composites.

The hybrid films comprising mixture of single-walled CNTs and WS_2 nanotubes with different volume fractions were fabricated and investigated in the microwave and terahertz ranges. It has been shown that both parameters g and g_0 decrease as the CNT volume fraction decreases. Opposite to polymer composite, the parameters g and g_0 remain large ($g > 25\%$, $g_0 > 75\%$) even at low CNT volume fraction (up to 1%) indicating strong EM interactions with CNTs within the hybrid films. This is due to the absence of the CNT agglomerates in these films.

The parameters g and g_0 can be used to estimate the quality of any other composite materials comprising conductive inclusions non-resonantly interacting with electromagnetic wave below 1 THz.

Acknowledgments

This research was partially supported by the Belarusian Republican Foundation for Fundamental Research (BRFFR) under project F15CO-016 and F17RM-068 the European Unions Seventh Framework Programme (FP7) for research, technological development and demonstration under projects FP7-612285 CANTOR, PIRSES-GA- 2012-318617. The work has also benefited of funding from the EU H2020 program under the MSCA-RISE-2014 project 644076 “CoExAN” and the MSCA-RISE-2016 project 734164 “Graphene-3D”. RT acknowledges the support of the H. Perlman foundation and the Irving and Azelle Waltcher Foundations in honour of Prof. M. Levy.

References

[1] Ugawa A., Rinzler A.G., Tanner D.B. Far-infrared gaps in single-wall carbon nanotubes. Phys Rev B1999;60(16):R11305–11308.

[2] Jeon T.I., Kim K.J., Kang C., Maeng I.H., Son J.H., An K.H., et al. Optical and electrical properties of preferentially anisotropic single-walled carbon-nanotube films in terahertz region. J Appl Phys2004;95(10):5736–40.

[3] Borondics F., Kamaras K., Nikolou M., Tanner D.B., Chen Z.H., Rinzler A.G. Charge dynamics in transparent single-walled carbon nanotube films from optical transmission measurements. Phys Rev B2006;74(4):045431.

[4] Slepyan G.Y., Shuba M.V., Maksimenko S.A., Thomsen C., Lakhtakia A. Terahertz conductivity peak in composite materials containing carbon nanotubes: Theory and interpretation of experiment. Phys Rev B2010;81(20):205423.

[5] Shuba M.V., Slepyan G.Y., Maksimenko S.A., Hanson G.W. Radiofrequency field absorption by carbon nanotubes embedded in a conductive host. J Appl Phys2010;108(11):114302.

[6] Zhang Q., Haroz E.H., Jin Z., Ren L., Wang X., Arvidson R.S., et al. Plasmonic nature of the terahertz conductivity peak in single-walled carbon nanotubes. Nano Lett2013;13:5991–6.

[7] Burke P.J. Luttinger liquid theory as a model of the gigahertz electrical properties of carbon nanotubes. IEEE Trans Nanotechnol2002;1(3):129–44.

[8] Slepyan G.Y., Maksimenko S.A., Lakhtakia A., Yevtushenko O., Gusakov A.V. Electrodynamics of carbon nanotubes: Dynamic conductivity, impedance boundary conditions, and surface wave propagation. Phys Rev B1999;60(24):17136–49.

[9] Shuba M.V., Paddubskaya A.G., Plyushch A.O., Kuzhir P.P., Slepyan G.Y., Maksimenko S.A., et al. Experimental evidence of localized plasmon resonance in composite materials containing single-wall carbon nanotubes. Phys Rev B2012;85:165435.

[10] Shuba M.V., Melnikov A.V., Paddubskaya A.G., Kuzhir P.P., Maksimenko S.A., Thomsen C. Role of finite-size effects in the microwave and subterahertz electromagnetic response of a multiwall carbon-nanotube-based composite: Theory and interpretation of experiments. Phys Rev B2013;88:045436.

[11] Shuba M.V., Paddubskaya A.G., Kuzhir P.P., Maksimenko S.A., Valusis G., Ivanov M., et al. Observation of the microwave near-field enhancement effect in suspensions comprising single-walled carbon nanotubes. Mat Research Express2017;4(7):075033.

[12] Bondarev I.V., Slepyan G.Y., Maksimenko S.A. Spontaneous decay of excited atomic states near a carbon nanotube. Phys Rev Lett2002;89:115504.

[13] Burke P.J., Li S., Yu Z. Quantitative theory of nanowire and nanotube antenna performance. IEEE Trans Nanotechnol2006;5(4):314–34.

[14] Hanson G. Fundamental transmitting properties of carbon nanotube antennas. IEEE Trans Antenn Propagat2005;53(11):3426–35.

[15] Slepyan G.Y., Shuba M.V., Maksimenko S.A., Lakhtakia A. Theory of optical scattering by achiral carbon nanotubes and their potential as optical nanoantennas. Phys Rev B2006;73(19):195416.

[16] Li H., Yin W.Y., Banerjee K., Mao J.F. Circuit modeling and performance analysis of multi-walled carbon nanotube interconnects. IEEE Trans Electon Dev2008;55(6):1328–37.

[17] Maffucci A., Miano G., Villone F. A new circuit model for carbon nanotube interconnects with diameter-dependent parameters. IEEE Trans Nanotechnol2009;8(3):345–54.

[18] Hartmann R.R., Kono J., Portnoi M.E. Terahertz science and technology of carbon nanomaterials. Nanotechnology2014;25(32):322001.

[19] Qin F., Brosseau C. A review and analysis of microwave absorption in polymer composites filled with carbonaceous particles. J Appl Phys2012;111(6):061301.

[20] Kuzhir P., Paddubskaya A., Bychanok D., Nemilentsau A., Shuba M., Plusch A., et al. Microwave probing of nanocarbon based epoxy resin composite films: Toward electromagnetic shielding. Thin Solid Films2011;519(12):4114–8.

[21] Bychanok D.S., Shuba M.V., Kuzhir P.P., Maksimenko S.A., Kubarev V.V., Kanygin M.A., et al. Anisotropic electromagnetic properties of polymer composites containing oriented multiwall carbon nanotubes in respect to terahertz polarizer applications. J Appl Phys2013;114(11):114304.

[22] Bauhofer W., Kovacs J.Z. A review and analysis of electrical percolation in carbon nanotube polymer composites. Comp Sci Techn2009;69(10):1486 –98.

[23] Kasaliwal G.R., Pegel S., Gldel A., Ptschke P., Heinrich G. Analysis of agglomerate dispersion mechanisms of multiwalled carbon nanotubes during melt mixing in polycarbonate. Polymer2010;51(12):2708–20.

[24] Noll A., Burkhart T. Morphological characterization and modelling of electrical conductivity of multi-walled carbon nanotube/poly(p-phenylene sulfide) nanocomposites obtained by twin screw extrusion. Comp Sci Technol2011;71(4):499 – 505.

[25] Kim S.W., Kim T., Kim Y.S., Choi H.S., Lim H.J., Yang S.J., et al. Surface modifications for the effective dispersion of carbon nanotubes in solvents and polymers. Carbon2012;50(1):3–33.

[26] Guadagno L., Vivo B.D., Bartolomeo A.D., Lamberti P., Sorrentino A., Tucci V., et al. Effect of functionalization on the thermo-mechanical and electrical behavior of multi-wall carbon nanotube/epoxy composites. Carbon2011;49(6):1919–30.

[27] Sahoo N.G., Rana S., Cho J.W., Li L., Chan S.H. Polymer nanocomposites based on functionalized carbon nanotubes. Prog Polym Sci2010;35(7):837 –67.

[28] Kotsilkova R., Ivanov E., Bychanok D., Paddubskaya A., Demidenko M., Macutkevic J., et al. Effects of sonochemical modification of carbon nanotubes on electrical and electromagnetic shielding properties of epoxy composites. Comp Sci Techn2015;106:85–92.

[29] Kranauskaite I., Macutkevic J., Banys J., Kuznetsov V.L., Moseenkov S.I., Rudyna N.A., et al. Length-dependent broadband electric properties of pmma composites filled with carbon nanotubes. Phys Stat Sol (a)2016;213(4):1025–33.

[30] Naffakh M., Diez-Pascual A.M., Gomez-Fatou M.A. New hybrid nanocomposites containing carbon nanotubes, inorganic fullerene-like ws2 nanoparticles and poly(ether ether ketone) (peek). J Mater Chem2011;21:7425–33.

[31] Hennrich F., Krupke R., Arnold K., Rojas Sttz J.A., Lebedkin S., Koch T., et al. The mechanism of cavitation-induced scission of single-walled carbon nanotubes. J Phys Chem B2007;111(8):1932–7.

[32] Peters O., Busch S.F., Fischer B.M., Koch M. Determination of the carbon nanotube concentration and homogeneity in resin films by thz spectroscopy and imaging. Int J Infr Mill Waves2012;33(12):1221–6.

[33] Casini R., Papari G., Andreone A., Marrazzo D., Patti A., Russo P. Dispersion of carbon nanotubes in melt compounded polypropylene based composites investigated by thz spectroscopy. Opt Express2015;23(14):18181–92.

[34] Durmus A., Kasgoz A., Macosko C.W. Linear low density polyethylene (lldpe)/clay nanocomposites. part i: Structural characterization and quantifying clay dispersion by melt rheology. Polymer2007;48(15):4492 –502.

[35] Morgan A.B., Gilman J.W. Characterization of polymer-layered silicate (clay) nanocomposites by transmission electron microscopy and x-ray diffraction: A comparative study. J Appl Polym Sci2003;87(8):1329–38.

[36] Blackburn J.L., Barnes T.M., Beard M.C., Kim Y.H., Tenent R.C., McDonald T.J., et al. Transparent conductive single-walled carbon nanotube networks with precisely tunable ratios of semiconducting and metallic nanotubes. ACS Nano2008;2(6):1266–74. PMID: 19206344.

[37] Shuba M.V., Maksimenko S.A., Slepyan G.Y. Absorption cross-section and near-field enhancement in finite-length carbon nanotubes in the terahertz-to-optical range. J Comput Theor Nanosci2009;6(9):2016–23.

[38] Bulmer J.S., Martens J., Kurzepa L., Gizewski T., Egilmez M., Blamire M.G., et al. Microwave conductivity of sorted cnt assemblies. Sci Rep2013;4:3762.

[39] Beard M.C., Blackburn J.L., Heben M.J. Photogenerated free carrier dynamics in metal and semiconductor single-walled carbon nanotube films. Nano Lett2008;8(12):4238–42.

[40] Wen B., Cao M.S., Hou Z.L., Song W.L., Zhang L., Lu M.M., et al. Temperature dependent microwave attenuation behavior for carbon-nanotube/silica composites. Carbon2013;65(Supplement C):124 –39. URL: http://www.sciencedirect.com/science/article/pii/S0008622313007689. doi:https://doi.org/10.1016/j.carbon.2013.07.110.

[41] Song W.L., Cao M.S., Hou Z.L., Fang X.Y., Shi X.L., Yuan J. High dielectric loss and its monotonic dependence of conducting-dominated multiwalled carbon nanotubes/silica nanocomposite on temperature ranging from 373 to 873 k in x-band. Applied Physics Letters2009;94(23):233110. URL: https://doi.org/10.1063/1.3152764. doi:10.1063/1.3152764. arXiv:https://doi.org/10.1063/1.3152764.

[42] Ran L., Xiao-Yong F., Yu-Qing K., Jie Y., Mao-Sheng C. Microwave absorption and response modeling of nanocomposites embedded sic nanoparticles. Chinese Physics Letters2009;26(4):044101. URL: http://stacks.iop.org/0256-307X/26/i=4/a=044101.

[43] Fang X.Y., Yu X.X., Zheng H.M., Jin H.B., Wang L., Cao M.S. Temperature- and thickness-dependent electrical conductivity of few-layer graphene and graphene nanosheets. Physics Letters A2015;379(37):2245 --51. URL: http://www.sciencedirect.com/science/article/pii/S0375960115005824. doi:https://doi.org/10.1016/j.physleta.2015.06.063.

[44] Karlsen P., Shuba M., Beckerleg C., Yuko D., Kuzhir P., Maksimenko S.A., et al. Influence of nanotube length and density on the plasmonic terahertz response of single-walled carbon nanotubes. Journal of Physics D: Applied Physics2017;URL: http://iopscience.iop.org/10.1088/1361-6463/aa96ef.

[45] Gorshunov B., Zhukova E., Starovatykh J., Belyanchikov M., Grebenko A., Bubis A., et al. Terahertz spectroscopy of charge transport in films of pristine and doped single-wall carbon nanotubes. Carbon2018;126(Supplement C):544 --51. URL: http://www.sciencedirect.com/science/article/pii/S0008622317310722. doi:https://doi.org/10.1016/j.carbon.2017.10.072.

[46] Wen B., Cao M., Lu M., Cao W., Shi H., Liu J., et al. Reduced graphene oxides: Light-weight and high-efficiency electromagnetic interference shielding at elevated temperatures. Advanced Materials2014;26(21):3484--9. URL: http://dx.doi.org/10.1002/adma.201400108. doi:10.1002/adma.201400108.

[47] Shuba M.V., Paddubskaya A.G., Kuzhir P.P., Maksimenko S.A., Flahaut E., Fierro V., et al. Short-length carbon nanotubes as building blocks for high dielectric constant materials in the terahertz range. J Phys D: Appl Phys2017;50(8):08LT01.

[48] Al-Saleh M.H., Saadeh W.H., Sundararaj U. Emi shielding effectiveness of carbon based nanostructured polymeric materials: A comparative study. Carbon2013;60:146 --56.

[49] Hennrich F., Lebedkin S., Malik S., Tracy J., Barczewski M., Rosner H., et al. Preparation, characterization and applications of free-standing single walled carbon nanotube thin films. Phys Chem Chem Phys2002;4:2273--7.

[50] Shuba M.V., Paddubskaya A.G., Kuzhir P.P., Maksimenko S.A., Ksenevich V.K., Niaura G., et al. Soft cutting of single-wall carbon nanotubes by low temperature ultrasonication in a mixture of sulfuric and nitric acids. Nanotechnology2012;23(49):495714.

[51] Gavrilov N., Okotrub A., Bulusheva L., Sedelnikova O., Yushina I., Kuznetsov V. Dielectric properties of polystyrene/onion-like carbon composites in frequency range of 0.5500khz. Comp Sci Techn2010;70(5):719--24.

[52] Zak A., Sallacan-Eecker L., Margolin A., Genut M., Tenne R. Insight into the growth mechanism of ws2 nanotubes in the scaled-up fluidized-bed reactor. Nano2009;04(02):91--8.

[53] Paddubskaya A., Valynets N., Kuzhir P., Batrakov K., Maksimenko S., Kotsilkova R., et al. Electromagnetic and thermal properties of three-dimensional printed multilayered nano-carbon/poly(lactic) acid structures. J Appl Phys2016;119(13):135102.

[54] Standard test method for measuring relative complex permittivity and relative magnetic permeability of solid materials at microwave frequencies, astm d5568-08. 2009.

[55] Chung B.K. Dielectric constant measurement for thin material at microwave frequencies. Progress In Electromagnetics Research2007;75:239. doi:10.2528/PIER07052801.

[56] Akima N., Iwasa Y., Brown S., Barbour A., Cao J., Musfeldt J., et al. Strong anisotropy in the far-infrared absorption spectra of stretch-aligned single-walled carbon nanotubes. Adv Mater2006;18(9):1166--9.

[57] Andreev A.S., ariya A. Kazakova , Ishchenko A.V., Selyutin A.G., Lapina O.B., Kuznetsov V.L., et al. Magnetic and dielectric

properties of carbon nanotubes with embedded cobalt nanoparticles. Carbon2017;114:39 -- 49.